

Universal van der Waals-type interactions in rattler containing cage materials

Jiazhen Wu,^{1,*} Jingtao Xu,² and Katsumi Tanigaki^{1,3,†}

¹WPI-AIMR, Tohoku University, Sendai, 980-8577, Japan

²Ningbo Institute of Materials Technology & Engineering, Chinese Academy of Sciences, Ningbo, China

³Graduate School of Science, Tohoku University, Sendai 980-8578, Japan

Rattling motion of fillers in cage materials has been of great interest for their import roles in superconductivity and thermoelectric applications. The standing waves of the rattling oscillations are normally lower in energy than the propagating waves of the acoustic phonons, thus exert large influences on the configuration of phonon dispersions as well as the associated thermal and electrical properties. Although it has been extensively studied, the origin of the low energy soft modes is still not clear. In the present paper, we show that van der Waals-type interactions are predominant between fillers and their surrounding cage frameworks, which explains the origin of the low energy modes in cage materials as a universal rule. Mass, free space and chemical environment of guest atoms are shown to be the most important factors to determine the three dimensional van der Waals-type interactions. The present work is mainly focused on type-I clathrates, skutterudites and pyrochlores.

PACS numbers:

Introduction

The rattling phenomenon might be first described by A. J. Sievers and S. Takeno in 1965, when they observed an anomalous peak of Li in KBr:LiBr at low frequencies.¹ Recently, rattling behavior has been commonly observed in filler containing cage materials, such as Al₁₀V-type intermetallides,² brownmillerite,³ skutterudite,⁴ pyrochlore⁵ and clathrate^{6,7}. Different from the Li-rattlers, the fillers (or guest atoms) in cage compounds are accommodated inside a periodic array of cages and can be quantitatively described. Fig. 1 shows a rattler containing cage, where the cage atoms are connected by covalent bonds, providing a strong wall and an oversized room for the guest atom. Since a guest atom is only weakly interacted with the surrounding cage atoms, it normally shows an anomalous low energy (ALE) frequency and a large atomic displacement parameter (ADP). Although showing anharmonicity, the ALE modes can be approximately described by the Einstein model, where guest atoms are treated as Einstein oscillators with a characteristic energy of ω_E . Rattling ALE phonon modes are scientifically important for: (1) their coupling with conduction electrons, giving rise to superconductivity^{5,8} and an modification of electron effective mass^{9,10}; and (2) their coupling with propagating phonons, leading to an enhancement of scattering probability and consequent low thermal conductivity for thermoelectric applications^{11,12}.

In the passed decades, the rattling phonon modes have been both experimentally and theoretically studied. The direct evidence has been provided by the phonon dispersion relationship of a type-I clathrate Ba₈Ga₁₆Ge₃₀, derived from inelastic neutron scattering measurements.⁷ The rattling phonon modes are optical-branch-like at around 5 meV, lower than the top of acoustic phonon branches, giving rise to ALE peaks in the derived phonon density of states (PDOS). The ALE vibration modes have also been detected and discussed by Raman spec-

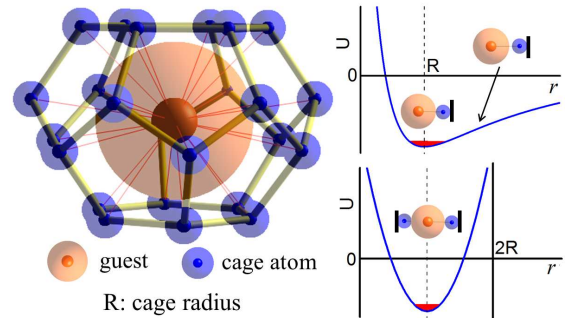


FIG. 1: Left: a sketched rattler containing cage. The cage atoms (hosts) are bonded via covalent interaction leaving enough room for the guest to move freely. The atomic radius of the guest atom is enlarged to illustrate the relatively large interspace. Right: sketched van der Waals potentials for a pair of guest-host atoms and a set of host-guest-host atoms. The later case is a simplified picture for a rattler containing cage.

troscopy,¹³ optical conductivity,¹⁴ heat capacity (HC),¹⁵ and temperature dependent ADP obtained from crystallographic refinement of x-ray/neutron diffraction data⁴. These experiment results have established the validity of the Einstein model for the description of the ALE modes; however exceptions were found for guest off-centered modes^{6,16} which were rather anharmonic and beyond the scope of the Einstein model and the present discussion. In addition, many theoretical investigations have been performed as well, aiming at unveiling the rattling phonon associated phonon static and dynamic properties.^{12,17} Nevertheless the origin of the low energy modes was not clear.

In our previous work,¹⁸ we addressed a van der Waals-type interaction between a filler and its surrounding cage framework as the origin of the rattling ALE modes by focusing only on the 6d parallel modes in type-I clathrates.

In the present study we extend our scope to the other two modes in type-I clathrates (2a and 6d perpendicular modes, refer to Fig. 2 for description of the modes) and the rattling modes in skutterudites and pyrochlores to unveil that the three dimensional (3D) van der Waals interaction is universal for rattler containing cage materials. Force constants, derived from the characteristic energies of guest atoms, are shown to vary exponentially with the free space of guest atoms (R_{free}) for each type of rattling mode. Different exponential parameters are obtained for different types of rattling modes, indicating that, besides space parameters discussed previously,¹⁸ chemical environment around guest atoms is another important factor that influences the guest-host interactions. The 3D van der Waals-type interaction, which coexists with the strong interatomic covalent interaction of framework atoms, significantly modifies the physical properties of a cage material via phonon-phonon and electron-phonon interactions, and provides a platform to study superconductivity and thermoelectricity.

Analyses method

A. Vibration modes and data collection

The current research is concerning the ALE vibration modes of the rattler in cage compounds. The situation for skutterudite and pyrochlore is simpler, because they are composed of single type of cages and have only one guest-vibration mode (as shown in Fig. 3). However, type-I clathrate, which contains two type of cages, is much more complicated. As shown in Fig. 2, there are three guest modes: 2a, 6d \parallel and 6d \perp modes, which are shown by the blue cage, black arrow and red arrow in the orange cage, respectively. Here 2a and 6d represent the crystallographic sites on the cage centers, \parallel and \perp are the directions with respect to the six-atom ring of the tetrakaidecahedral cage.

Different ALE modes have different characteristic energies (ω_E), depending on the chemical environment and the relative free space that rattlers can move. In principle, the vibration energies can be directly detected by INS, Raman spectroscopy and heat capacity measurements. However, if ω_E is not low enough, and close to the top of an acoustic phonon branch, where the acoustic phonon becomes less propagative (the acoustic phonon branch becomes flat at the Brillouin zone edge), ω_E cannot be precisely obtained from these experiment techniques, because the contributions from van Hove singularities cannot be extracted. We have exemplified the situation in the heat capacity analyses for $\text{K}_8\text{Ga}_8\text{Sn}_{38}$, where the number of ALE modes obtained from data fitting exceeds what we expect from the number of guest atoms, showing clearly the contributions from van Hove singularities.¹⁸ In order to obtain a correct value for ω_E , temperature dependent ADP of a guest atom is useful.⁴ Therefore, the ω_E 's in the present analyses are mainly

derived from ADP data from literatures (Refs.¹⁹⁻⁴¹) for the three modes of type-I clathrates and the guest modes of skutterudites. The ω_E 's for pyrochlores are taken from heat capacity data reported by Hiroi *et. al.*⁴² The data are summarized in table I.

B. Van der Waals potential model and harmonic approximation

To interpret the guest vibration modes, we introduce a modified Morse potential as we did previously.^{18,45} As shown in Fig. 1, the potential of a guest atom inside a cage can be simplified by pair-wise potentials and expressed by,

$$\begin{aligned} V_t(r) &= V(R+r) + V(R-r) \\ &= ae^{-nb(R+r-r_e)} - ane^{-b(R+r-r_e)} \\ &\quad + ae^{-nb(R-r-r_e)} - ane^{-b(R-r-r_e)} \end{aligned} \quad (1)$$

where R is shown in Fig. 1 and can be viewed as a cage radius, r_e is the equilibrium distance and can be estimated by $R_{\text{guest}} + R_{\text{host}}$ using van der radii of atoms; n , a and b are free parameters with $n \gg 1$. The expression can be simplified by introducing $R_{\text{free}} = R - r_e$:

$$\begin{aligned} V_t(r) &= ae^{-nb(R_{\text{free}}+r)} - ane^{-b(R_{\text{free}}+r)} \\ &\quad + ae^{-nb(R_{\text{free}}-r)} - ane^{-b(R_{\text{free}}-r)} \end{aligned} \quad (2)$$

What we are focusing on is the potential minimum, where a guest atom is on the center and r equals to zero. One can easily derive the following equations,

$$V_t(r=0) = 2a(e^{-nbR_{\text{free}}} - ne^{-bR_{\text{free}}}) \quad (3)$$

$$V_t'(r=0) = 0 \quad (4)$$

$$V_t''(r=0) = 2anb^2(ne^{-nbR_{\text{free}}} - e^{-bR_{\text{free}}}) \quad (5)$$

A potential minimum requires $V_t'' > 0$, so the cage radius should satisfy the following criteria,

$$R < R_c = r_e + \frac{\ln(n)}{nb - b}. \quad (6)$$

otherwise, the central position is not stable, and two potential minima arise near the center.

Under harmonic approximation, the force constant (Fc) of a harmonic oscillator can be expressed by $V_t''(r=0)$, with the assumption that the repulsive term is much larger than the attractive term.

$$\begin{aligned} Fc &= 2anb^2(ne^{-nbR_{\text{free}}} - e^{-bR_{\text{free}}}) \\ &\cong 2an^2b^2e^{-nbR_{\text{free}}} \end{aligned} \quad (7)$$

Experimentally, Fc can be estimated by the harmonic oscillator model that $Fc = m\omega_E^2$. Therefore, the simple exponential relationship can be tested by experiment data.

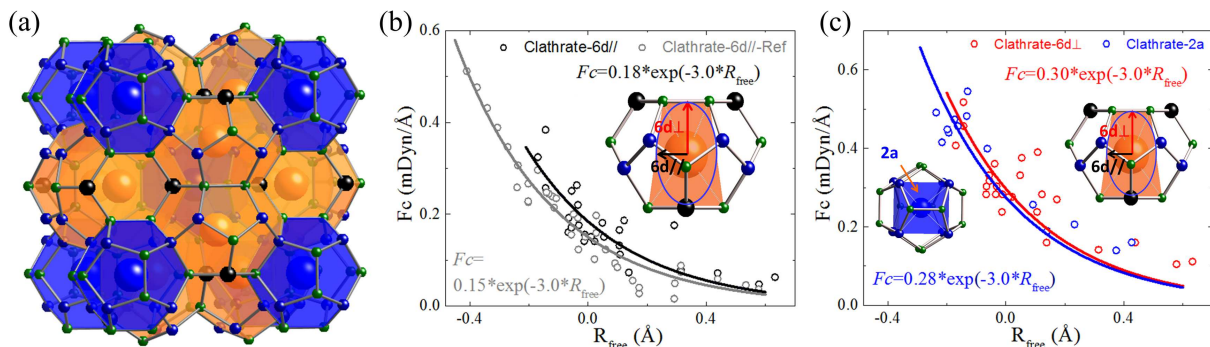


FIG. 2: (a) lattice structure of type-I clathrate. The cage framework is mainly composed of Si/Ge/Sn and the colors of the atoms indicate different crystallographic sites. The guest atoms are alkali metals or alkaline earth metals. There are two types of cages, dodecahedral and tetrakaidecahedral cages, which are shown by blue and orange colors, respectively. (b,c) The relationship between F_c and R_{free} for different vibration modes in type-I clathrates. The closest interspaces between guest and cage atoms are shown in the inset of the figures for both types of cages. The arrows show anisotropic vibration modes (6d modes) in the tetrakaidecahedral cage. The lines are fitting results by employing exponential functions. The original data are derived from Refs.,^{19–38} and the data with grey color is taken from our previous work.¹⁸

C. Unified picture of different ALE modes in cage compounds

As shown in Fig.2(b-c), the exponential behavior, $F_c = Ae^{-BR_{\text{free}}}$, holds for each guest mode in type-I clathrate. Here $A = 2an^2b^2$ and $B = nb$, corresponding to the parameters derived earlier. R_{free} was estimated using $R_{\text{free}} = R - R_{\text{guest}} - R_{\text{host}}$, and R was defined as the distance between a guest atom and its nearest neighbour.^{10,18} van der Waals radii were used for R_{guest} and R_{host} ^{18,46,47} and they are: 1.40 Å(Sr), 1.57 Å(Ba), 1.01 Å(Na), 1.32 Å(K), 1.44 Å(Rb), 1.61 Å(Cs), 1.27 Å(Ca), 2.10 Å(Si), 2.11 Å(Ge), 2.17 Å(Sn), 1.87 Å(Ga), 1.39 Å(Zn), 1.4 Å(Cu), 1.63 Å(Ni), 1.72 Å(Ag), 1.66 Å(Au), 1.58 Å(Cd), 1.93 Å(In), 1.84 Å(Al), 1.52 Å(O) and 2.06 Å(Sb). Irrespective of different vibration modes, the component elements are same for different cages, therefore we assume nb keeps the same value for each case, and a is variant depending on the effective number of guest-host pairs (the total potential is the sum of the component pairwise potentials). In the fitting, we set $B = 3.0$, which we reported previously¹⁸. The fitting parameters A and B are listed in Table II. For the 6d|| mode, the result from ADP data is consistent with the result from heat capacity data¹⁸. The 2a and 6d⊥ modes show similar behavior but are much stronger than the 6d|| mode. The difference will be discussed later on, but it is noteworthy that it does not originate from space parameters, which have been already renormalized by R_{free} .

For skutterudite and pyrochlore, although lack of sufficient data point, the exponential dependence can also be clearly seen in Fig.3(b-c). Obviously, the guest-host interaction is much stronger than that in type-I clathrate, this might be the reason that rattling vibrations in some of these compounds have much higher energies and can

not be clearly distinguished from other high energy non-dispersive phonon modes.^{48,49}

Discussion

To have a deep insight into the guest-host interactions based on the van der Waals potential model, we consider the nearest cage atoms as primary atoms that strongly interact with the guest atom. The closest interspace for each cage is shown in Fig.2 and Fig.3. In type-I clathrate, for both dodecahedral and tetrakaidecahedral cages, guest atoms have eight nearest neighbors; however the closest interspaces are in different shapes: a cube and a twisted cuboid, respectively. Therefore the 2a mode inside the cube is isotropic, while the 6d mode inside the twisted cuboid is anisotropic and splits into a 6d|| mode and a 6d⊥ mode. The total guest-host interactions inside the tetrakaidecahedral cage can be resolved along 6d|| and 6d⊥ directions, as shown by the arrows in Fig.2(b-c). According to the geometry of the twisted cuboid, the strength of the interaction along 6d|| direction is weaker than that along 6d⊥ direction, and the ratio is around 0.62, which is very close to the ratio of the fitting parameters (shown in table II), $A_{6d||}/A_{6d⊥} \cong 0.6$. This is not just a coincidence, but rather indicates that the proposed van der Waals interaction works well for the rattling system, and the interaction is closely associated with the effective number of pairwise potentials (or the coordination number) and the cage geometry.

In skutterudite and pyrochlore, the situation is very different, not only in the number and geometry of the primary cage atoms, but also in the component elements. Correspondingly, the fitting parameters A and B are very different. The cage of clathrate is mainly composed of Si/Ge/Sn, while the cage of skutterudite is mainly composed of P/As/Sb and the cage of pyrochlore is mainly

TABLE I: The values of ω_E for the present analyses.

| compounds | vibration modes | ω_E (K) | Ref. | compounds | vibration modes | ω_E (K) | Ref. |
|---|-----------------|----------------|-------------------|--|-----------------|----------------|-------------------|
| Type-I Clathrate | | | | | | | |
| Ba ₈ Al ₁₆ Si ₃₀ | Ba(6d) | 68 | ADP ²⁸ | Ba ₈ Al ₁₆ Ge ₃₀ | Ba(6d) | 69 | ADP ¹⁹ |
| Ba ₈ Al ₁₆ Si ₃₀ | Ba(6d⊥) | 92 | ADP ²⁸ | Ba ₈ Al ₁₆ Ge ₃₀ | Ba(6d⊥) | 85 | ADP ¹⁹ |
| Ba ₈ Al ₁₆ Si ₃₀ | Ba(2a) | 111 | ADP ²⁸ | Ba ₈ Al ₁₆ Ge ₃₀ | Ba(2a) | 101 | ADP ¹⁹ |
| Ba ₈ Zn ₇ Si ₃₉ | Ba(6d) | 80 | ADP ²⁹ | Ba ₈ Ni ₆ Ge ₄₀ | Ba(6d) | 75 | ADP ²⁸ |
| Ba ₈ Zn ₇ Si ₃₉ | Ba(6d⊥) | 90 | ADP ²⁹ | Ba ₈ Ni ₆ Ge ₄₀ | Ba(6d⊥) | 85 | ADP ²⁸ |
| Ba ₈ Ga ₁₆ Si ₃₀ | Ba(6d) | 66 | ADP ²⁸ | Ba ₈ Ni ₆ Ge ₄₀ | Ba(2a) | 103 | ADP ²⁸ |
| Ba ₈ Ga ₁₆ Si ₃₀ | Ba(6d⊥) | 92 | ADP ²⁸ | Ba ₈ Cu ₆ Ge ₄₀ | Ba(6d) | 63 | ADP ²¹ |
| Ba ₈ Ga ₁₆ Si ₃₀ | Ba(2a) | 112 | ADP ²⁸ | Ba ₈ Cu ₆ Ge ₄₀ | Ba(6d⊥) | 85 | ADP ²¹ |
| Ba ₈ Rh _{2.4} Si _{43.6} | Ba(6d) | 99 | ADP ³¹ | Ba ₈ Cu ₆ Ge ₄₀ | Ba(2a) | 106 | ADP ²¹ |
| Ba ₈ Rh _{2.4} Si _{43.6} | Ba(6d⊥) | 115 | ADP ³¹ | Ba ₈ Zn ₈ Ge ₃₈ | Ba(6d) | 62 | ADP ²² |
| Ba ₈ Ag ₅ Si ₄₁ | Ba(6d) | 81 | ADP ⁴³ | Ba ₈ Zn ₈ Ge ₃₈ | Ba(6d⊥) | 98 | ADP ²² |
| Ba ₈ Ag ₅ Si ₄₁ | Ba(6d⊥) | 108 | ADP ⁴³ | Ba ₈ Zn ₈ Ge ₃₈ | Ba(2a) | 118 | ADP ²² |
| Ba ₈ Ni ₃ Si ₄₃ | Ba(6d) | 91 | ADP ³² | Ba ₈ Ga ₁₆ Ge ₃₀ | Ba(6d) | 60 | ADP ²³ |
| Ba ₈ Ni ₃ Si ₄₃ | Ba(6d⊥) | 102 | ADP ³² | Ba ₈ Ga ₁₆ Ge ₃₀ | Ba(6d⊥) | 84 | ADP ²³ |
| Na ₈ Si ₄₆ | Na(6d) | 110 | ADP ³⁵ | Ba ₈ Ga ₁₆ Ge ₃₀ | Ba(2a) | 108 | ADP ²³ |
| Na ₈ Si ₄₆ | Na(6d⊥) | 147 | ADP ³⁵ | Ba ₈ Rh _{1.2} Ge _{42.8} | Ba(6d) | 70 | ADP ²⁴ |
| Na ₈ Si ₄₆ | Na(2a) | 170 | ADP ³⁵ | Ba ₈ Rh _{1.2} Ge _{42.8} | Ba(6d⊥) | 88 | ADP ²⁴ |
| Sr ₈ Al ₁₁ Si ₃₅ | Sr(6d) | 67 | ADP ¹⁵ | Ba ₈ Ag ₆ Ge ₄₀ | Ba(6d) | 60 | ADP ²¹ |
| Sr ₈ Al ₁₁ Si ₃₅ | Sr(6d⊥) | 125 | ADP ¹⁵ | Ba ₈ Ag ₆ Ge ₄₀ | Ba(6d⊥) | 78 | ADP ²¹ |
| Sr ₈ Al ₆ Ga ₁₀ Si ₃₀ | Sr(6d) | 54 | ADP ³⁸ | Ba ₈ Ag ₆ Ge ₄₀ | Ba(2a) | 107 | ADP ²¹ |
| Sr ₈ Al ₆ Ga ₁₀ Si ₃₀ | Sr(6d⊥) | 80 | ADP ³⁸ | Ba ₈ Cd _{7.6} Ge _{38.4} | Ba(6d) | 58 | ADP ²⁸ |
| Ba ₈ Ga ₁₆ Sn ₃₀ | Ba(6d⊥) | 67 | ADP ³³ | Ba ₈ Cd _{7.6} Ge _{38.4} | Ba(6d⊥) | 78 | ADP ²⁸ |
| Ba ₈ Ga ₁₆ Sn ₃₀ | Ba(2a) | 81 | ADP ³³ | Ba ₈ In ₁₆ Ge ₃₀ | Ba(6d) | 65 | ADP ²⁶ |
| K ₈ Ga ₈ Sn ₃₈ | K(6d) | 65 | ADP ³⁴ | Ba ₈ Ir _{0.2} Ge _{43.2} | Ba(6d) | 64 | ADP ³¹ |
| K ₈ Ga ₈ Sn ₃₈ | K(6d⊥) | 97 | ADP ³⁴ | Ba ₈ Ir _{0.2} Ge _{43.2} | Ba(6d⊥) | 85 | ADP ³¹ |
| K ₈ Ga ₈ Sn ₃₈ | K(2a) | 112 | ADP ³⁴ | Ba ₈ Pt _{2.7} Ge _{41.7} | Ba(6d) | 82 | ADP ²⁷ |
| K ₈ Zn ₄ Sn ₄₂ | K(6d) | 78 | ADP ⁴⁴ | Ba ₈ Pt _{2.7} Ge _{41.7} | Ba(6d⊥) | 96 | ADP ²⁷ |
| K ₈ Zn ₄ Sn ₄₂ | K(6d⊥) | 97 | ADP ⁴⁴ | Ba ₈ Au ₆ Ge ₄₀ | Ba(6d) | 62 | ADP ²¹ |
| K ₈ Zn ₄ Sn ₄₂ | K(2a) | 120 | ADP ⁴⁴ | Ba ₈ Au ₆ Ge ₄₀ | Ba(6d⊥) | 84 | ADP ²¹ |
| Rb ₈ Sn ₄₄ | Rb(6d) | 54 | ADP ³⁷ | Ba ₈ Au ₆ Ge ₄₀ | Ba(2a) | 110 | ADP ²¹ |
| Rb ₈ Sn ₄₄ | Rb(6d⊥) | 81 | ADP ³⁷ | Sr ₈ Ga ₁₆ Ge ₃₀ | Sr(6d) | 80 | ADP ²⁶ |
| Rb ₈ Sn ₄₄ | Rb(2a) | 92 | ADP ³⁷ | Sr ₈ Ga ₁₆ Ge ₃₀ | Sr(6d⊥) | 104 | ADP ²⁶ |
| Skutterudite | | | | | | | |
| NaFe ₄ Sb ₁₂ | Na | 162 | ADP ³⁹ | CaFe ₄ Sb ₁₂ | Ca | 114 | ADP ³⁹ |
| SrFe ₄ Sb ₁₂ | Sr | 113 | ADP ³⁹ | BaFe ₄ Sb ₁₂ | Ba | 126 | ADP ³⁹ |
| Pyrochlore | | | | | | | |
| KOs ₂ O ₆ | K | 61 | HC ⁴² | RbOs ₂ O ₆ | Rb | 66 | HC ⁴² |
| CsOs ₂ O ₆ | Cs | 75 | HC ⁴² | | | | |

composed of O. The elements in the later cases have much large electronegativity, which may introduce additional interactions, such as ionic interactions, in addition to the principal van der Waals interactions. Under such an assumption, the guest atoms should be more easily to be off-

centered, and this is true for pyrochlore compounds,^{42,50} while skutterudite cages are usually very small, so off-centered guest atoms were rarely observed. This conclusion can be supported by the critical radius estimated earlier as shown in equation 6. The large $nb(B)$ values

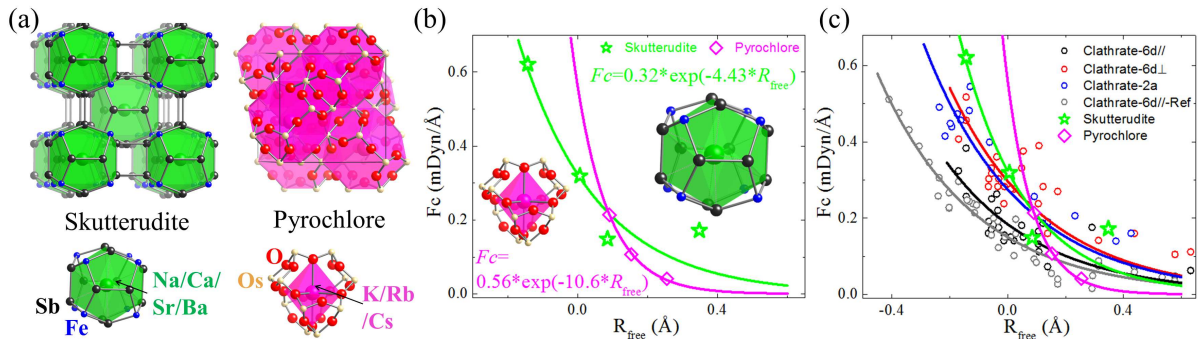


FIG. 3: (a) lattice structures of a typical skutterudite and pyrochlore, their cages are shown by green and pink colors, respectively. The closest interspaces between guest and cage atoms are shown for both compounds. (b) The relationship between F_c and R_{free} for different vibration modes of guest atoms in skutterudites and pyrochlores. The lines are fitting results by employing exponential functions, and their colors are corresponding to the colors of cages. The data of skutterudite and pyrochlore are derived from Refs. ^{39,42} (c) A summary for clathrates, skutterudites and pyrochlores.

TABLE II: Fitting parameters of the relationship between F_c and R_{free} . $F_c = Ae^{-BR_{\text{free}}}$.

| vibration modes | A | B |
|---|------|------|
| clathrate-2a | 0.28 | 3.0 |
| clathrate-6d \perp | 0.30 | 3.0 |
| clathrate-6d \parallel | 0.18 | 3.0 |
| clathrate-6d \parallel -ref ¹⁸ | 0.15 | 3.0 |
| Skutterudite | 0.32 | 4.4 |
| Pyrochlore | 0.56 | 10.6 |

for skutterudite and pyrochlore would give rise to a small R_c , and it is readily for a cage to be oversized and the guest atom becomes off-centered.

Conclusions

In the present work, we studied the ALE vibration modes of guest atoms in cage materials by focusing on type-I clathrates, skutterudites and pyrochlores. We showed that the 3D van der Waals-type interaction,

which is usually important only in molecular solids but negligible in the other types of solids (ionic, covalent, etc.), can be clearly observed in cage compounds with strong covalent framework. The strong covalent bonded cages create a solid wall and chemical pressure between guest atoms and their surrounding frameworks, stabilizing the anomalous low energy phonon modes. In addition to free space and mass parameters, which we derived previously¹⁸, we introduced another three chemical environment associated factors: (1) coordination number of guest atoms, or the effective number of pairwise potentials; (2) geometry of cages; (3) electronegativity of the component elements of a cage. These five factors work together to determine the interesting soft modes of the rattling vibrations. The 3D van der Waals-type interaction in cage materials should be highly evaluated in the community of superconductivity and thermoelectricity.

Acknowledgment

This work was partially supported by the AIMR collaborative research program. JX acknowledges the financial support by the National Nature Science Foundation of China (NSFC No. 11304327).

* wujzphystu@gmail.com

† tanikagi@sspns.phys.tohoku.ac.jp

¹ A. J. Sievers and S. Takeno. Isotope Shift of a Low-Lying Lattice Resonant Mode. *Phys. Rev.*, 140:A1030–A1032, 1965.

² A. D. Caplin, G. Grüner, and J. B. Dunlop. Al₁₀V: An Einstein Solid. *Phys. Rev. Lett.*, 30:1138–1140, 1973.

³ A. I. Rykov, K. Nomura, T. Mitsui, and M. Seto. Low-energy excitations in brownmillerites and related oxides. *Physica B: Condensed Matter*, 350(4):287–304, 2004. ISSN 0921-4526.

⁴ B. C. Sales, D. Mandrus, B. C. Chakoumakos, V. Keppens, and J. R. Thompson. Filled skutterudite antimonides: Electron crystals and phonon glasses. *Phys. Rev. B*, 56: 15081–15089, 1997.

⁵ Z. Hiroi, S. Yonezawa, Y. Nagao, and J. Yamaura. Extremely strong-coupling superconductivity and anomalous lattice properties in the β -pyrochlore oxide KO₂O₆. *Phys. Rev. B*, 76:014523, 2007.

⁶ B. C. Sales, B. C. Chakoumakos, R. Jin, J. R. Thompson, and D. Mandrus. Structural, magnetic, thermal, and transport properties of X₈Ga₁₆Ge₃₀ (X = Eu, Sr, Ba) sin-

- gle crystals. *Phys. Rev. B*, 63:245113, 2001.
- 7 M. Christensen, A. B. Abrahamsen, N. B. Christensen, F. Juranyi, N. H. Andersen, K. Lefmann, J. Andreasson, C. R. H. Bahl, and B. B. Iversen. Avoided crossing of rattler modes in thermoelectric materials. *Nature Materials*, 7:811–815, 2008.
 - 8 Shoji Yamanaka, Eiji Enishi, Hiroshi Fukuoka, and Masahiro Yasukawa. High-Pressure Synthesis of a New Silicon Clathrate Superconductor, $\text{Ba}_8\text{Si}_{46}$. *Inorganic Chemistry*, 39:56–58, 2000.
 - 9 Jingtao Xu, Jun Tang, Kazumi Sato, Yoichi Tanabe, Hitoshi Miyasaka, Masahiro Yamashita, Satoshi Heguri, and Katsumi Tanigaki. Low-temperature heat capacity of $\text{Sr}_8\text{Ga}_{16}\text{Ge}_{30}$ and $\text{Ba}_8\text{Ga}_{16}\text{Ge}_{30}$: Tunneling states and electron-phonon interaction in clathrates. *Phys. Rev. B*, 82:085206, 2010.
 - 10 Jiazhen Wu, Jingtao Xu, Dwi Prananto, Hidekazu Shimotani, Yoichi Tanabe, Satoshi Heguri, and Katsumi Tanigaki. Systematic studies on anharmonicity of rattling phonons in type-I clathrates by low-temperature heat capacity measurements. *Phys. Rev. B*, 89:214301, 2014.
 - 11 J. L. Cohn, G. S. Nolas, V. Fessatidis, T. H. Metcalf, and G. A. Slack. Glasslike Heat Conduction in High-Mobility Crystalline Semiconductors. *Phys. Rev. Lett.*, 82:779–782, 1999.
 - 12 Terumasa Tadano, Yoshihiro Gohda, and Shinji Tsuneyuki. Impact of Rattlers on Thermal Conductivity of a Thermoelectric Clathrate: A First-Principles Study. *Phys. Rev. Lett.*, 114:095501, 2015.
 - 13 Tetsuji Kume, Hiroshi Fukuoka, Toshihiro Koda, Shigeo Sasaki, Hiroyasu Shimizu, and Shoji Yamanaka. High-Pressure Raman Study of Ba Doped Silicon Clathrate. *Phys. Rev. Lett.*, 90:155503, 2003.
 - 14 T. Mori, S. Goshima, K. Iwamoto, S. Kushibiki, H. Matsumoto, N. Toyota, K. Suekuni, M. A. Avila, T. Takabatake, T. Hasegawa, N. Ogita, and M. Udagawa. Optical conductivity of rattling phonons in type-I clathrate $\text{Ba}_8\text{Ga}_{16}\text{Ge}_{30}$. *Phys. Rev. B*, 79:212301, 2009.
 - 15 Toshiro Takabatake, Koichiro Suekuni, Tsuneyoshi Nakayama, and Eiji Kaneshita. Phonon-glass electron-crystal thermoelectric clathrates: Experiments and theory. *Rev. Mod. Phys.*, 86:669–716, 2014.
 - 16 K. Suekuni, M. A. Avila, K. Umeo, H. Fukuoka, S. Yamanaka, T. Nakagawa, and T. Takabatake. Simultaneous structure and carrier tuning of dimorphic clathrate $\text{Ba}_8\text{Ga}_{16}\text{Sn}_{30}$. *Phys. Rev. B*, 77:235119, 2008.
 - 17 T. Nakayama and E. Kanashita. Interacting dipoles in typ-I clathrates: Why glass-like though crystalline? *EPL (Europhysics Letters)*, 84(6):66001, 2008.
 - 18 J. Wu, K. Akagi, J. Xu, H. Shimotani, K. K. Huynh, and K. Tanigaki. Unification of the low-energy excitation peaks in the heat capacity that appears in clathrates. *Phys. Rev. B*, 93:094303, 2016.
 - 19 M. Christensen and B. B. Iversen. Host Structure Engineering in Thermoelectric Clathrates. *Chem. Mater*, 19(20):4896–4905, 2007.
 - 20 Simon Johnsen, Anders Bentien, Georg K. H. Madsen, Mats Nygren, and Bo B. Iversen. Crystal structure and transport properties of nickel containing germanium clathrates. *Phys. Rev. B*, 76:245126, 2007.
 - 21 S. Johnsen, M. Christensen, B. Thomsen, G. K. H. Madsen, and B. B. Iversen. Barium dynamics in noble-metal clathrates. *Phys. Rev. B*, 82:184303, 2010.
 - 22 M. Christensen and B. B. Iversen. Hostguest coupling in semiconducting $\text{Ba}_8\text{Zn}_8\text{Ge}_{38}$. *Journal of Physics: Condensed Matter*, 20(10):104244, 2008.
 - 23 Mogens Christensen, Nina Lock, Jacob Overgaard, and Bo B. Iversen. Crystal Structures of Thermoelectric n- and p-type $\text{Ba}_8\text{Ga}_{16}\text{Ge}_{30}$ Studied by Single Crystal, Multitemperature, Neutron Diffraction, Conventional X-ray Diffraction and Resonant Synchrotron X-ray Diffraction. *Journal of the American Chemical Society*, 128(49):15657–15665, 2006.
 - 24 M. Falmbigl, F. Kneidinger, M. Chen, A. Grytsiv, H. Michor, E. Royanian, E. Bauer, H. Effenberger, R. Podloucky, and P. Rogl. Cage-Forming Compounds in the BaRhGe System: From Thermoelectrics to Superconductivity. *Inorganic Chemistry*, 52(2):931–943, 2013.
 - 25 I. Zeiringer, M. Chen, I. Bednar, E. Royanian, E. Bauer, R. Podloucky, A. Grytsiv, P. Rogl, and H. Effenberger. Phase Equilibria, Crystal Chemistry and Physical Properties of Au-Ba-Ge Clathrates. *Acta Materialia*, 59:2368–2384, 2011.
 - 26 A. Bentien, E. Nishibori, S. Paschen, and B. B. Iversen. Crystal structures, atomic vibration, and disorder of the type-I thermoelectric clathrates $\text{Ba}_8\text{Ga}_{16}\text{Si}_{30}$, $\text{Ba}_8\text{Ga}_{16}\text{Ge}_{30}$, $\text{Ba}_8\text{In}_{16}\text{Ge}_{30}$, and $\text{Sr}_8\text{Ga}_{16}\text{Ge}_{30}$. *Phys. Rev. B*, 71:144107, 2005.
 - 27 N. Melnychenko-Koblyuk, A. Grytsiv, P. Rogl, M. Rotter, R. Lackner, E. Bauer, L. Fornasari, F. Marabelli, and G. Giester. Structure and physical properties of type-I clathrate solid-solution $\text{Ba}_8\text{Pt}_x\text{Ge}_{46-x-y}\text{V}_y$ (V = vacancy). *Phys. Rev. B*, 76:195124, 2007.
 - 28 Mogens Christensen, Simon Johnsen, and Bo Brummerstedt Iversen. Thermoelectric clathrates of type I. *Dalton Trans.*, 39:978–992, 2010.
 - 29 N. Nasir, A. Grytsiv, N. Melnychenko-Koblyuk, P. Rogl, E. Bauer, R. Lackner, E. Royanian, G. Giester, and A. Saccone. Clathrates $\text{Ba}_8(\text{Zn,Cd})_x\text{Si}_{46x}$, $x \sim 7$: synthesis, crystal structure and thermoelectric properties. *Journal of Physics: Condensed Matter*, 21(38):385404, 2009.
 - 30 A. Bentien, B. B. Iversen, J. D. Bryan, G. D. Stucky, A. E. C. Palmqvist, A. J. Schultz, and R. W. Henning. Maximum entropy method analysis of thermal motion and disorder in thermoelectric clathrate $\text{Ba}_8\text{Ga}_{16}\text{Si}_{30}$. *Journal of Applied Physics*, 91(9):5694–5699, 2002.
 - 31 M. Falmbigl, A. Grytsiv, P. Rogl, and G. Giester. Clathrate formation in the systems BaIrGe and $\text{Ba}(\text{Rh,Ir})\text{Si}$: Crystal chemistry and phase relations. *Intermetallics*, 36:61–72, 2013.
 - 32 M. Falmbigl, M. X. Chen, A. Grytsiv, P. Rogl, E. Royanian, H. Michor, E. Bauer, R. Podloucky, and G. Giester. Type-I clathrate $\text{Ba}_8\text{Ni}_x\text{Si}_{46-x}$: Phase relations, crystal chemistry and thermoelectric properties. *Dalton Trans.*, 41:8839–8849, 2012.
 - 33 Sebastian Christensen, Marcos A. Avila, Koichiro Suekuni, Ross Piltz, Toshiro Takabatake, and Mogens Christensen. Combined X-ray and neutron diffraction study of vacancies and disorder in the dimorphic clathrate $\text{Ba}_8\text{Ga}_{16}\text{Sn}_{30}$ of type I and VIII. *Dalton Trans.*, 42:14766–14775, 2013.
 - 34 T. Tanaka, T. Onimaru, K. Suekuni, S. Mano, H. Fukuoka, S. Yamanaka, and T. Takabatake. Interplay between thermoelectric and structural properties of type-I clathrate $\text{K}_8\text{Ga}_8\text{Sn}_{38}$ single crystals. *Phys. Rev. B*, 81:165110, 2010.
 - 35 S. Stefanoski, J. Martin, and G. S. Nolas. Low temperature transport properties and heat capacity of single-crystal $\text{Na}_8\text{Si}_{46}$. *J. Phys. Condens. Matter*, 22:485404, 2010.
 - 36 J. H. Roudebush, N. Tsujii, A. Hurtando, H. Hope,

- Yu. Grin, and S. M. Kauzlarich. Phase Range of the Type-I Clathrate $\text{Sr}_8\text{Al}_x\text{Si}_{46-x}$ and Crystal Structure of $\text{Sr}_8\text{Al}_{10}\text{Si}_{36}$. *Inorganic Chemistry*, 51(7):4161–4169, 2012.
- ³⁷ Andreas Kaltzoglou, Thomas Fassler, Mogens Christensen, Simon Johnsen, Bo Iversen, Igor Presniakov, Alexey Sobolev, and Andrei Shevelkov. Effects of the order-disorder phase transition on the physical properties of A_8Sn_{44} ($\text{A} = \text{Rb}, \text{Cs}$). *J. Mater. Chem.*, 18:5630–5637, 2008.
- ³⁸ H. Shimizu, Y. Takeuchi, T. Kume, S. Sasaki, K. Kishimoto, N. Ikeda, and T. Koyanagi. Raman spectroscopy of type-I and type-VIII silicon clathrate alloys $\text{Sr}_8\text{Al}_x\text{Ga}_{16-x}\text{Si}_{30}$. *Journal of Alloys and Compounds*, 487(12):47–51, 2009.
- ³⁹ W. Schnelle, A. Leithe-Jasper, H. Rosner, R. Cardoso-Gil, R. Gumeniuk, D. Trots, J. A. Mydosh, and Yu. Grin. Magnetic, thermal, and electronic properties of iron-antimony filled skutterudites $M\text{Fe}_4\text{Sb}_{12}$ ($M = \text{Na}, \text{K}, \text{Ca}, \text{Sr}, \text{Ba}, \text{La}, \text{Yb}$). *Phys. Rev. B*, 77:094421, 2008.
- ⁴⁰ J. Xu, J. Wu, H. Shao, S. Heguri, Y. Tanabe, Y. Liu, G. Liu, J. Jiang, H. Jiang, and K. Tanigaki. Structure and thermoelectric properties of the n-type clathrate $\text{Ba}_8\text{Cu}_{5.1}\text{Ge}_{40.2}\text{Sn}_{0.7}$. *Journal of Materials Chemistry A*, 3:19100, 2015.
- ⁴¹ J. Xu, J. Wu, S. Heguri, G. Mu, Y. Tanabe, and K. Tanigaki. Low-temperature physical properties of $\text{Ba}_8\text{Ni}_x\text{Ge}_{46-x}$ ($x = 3, 4, 6$). *Journal of Electronic Materials*, 41(6):1177–1180, 2012.
- ⁴² Zenji Hiroi, Jun-ichi Yamaura, and Kazumasa Hattori. Rattling Good Superconductor: β -Pyrochlore Oxides AOs_2O_6 . *Journal of the Physical Society of Japan*, 81(1):011012, 2012.
- ⁴³ I. Zeiringer, E. Bauer, A. Grytsiv, P. Rogl, and H. Effenberger. Phase Equilibria, Crystal Chemistry, and Physical Properties of AgBaSi Clathrates. *Jpn. J. Appl. Phys.*, 50:05FA01, 2011.
- ⁴⁴ J. Xu, J. Wu, S. Heguri, Y. Tanabe, G. Liu, J. Jiang, H. Jiang, and K. Tanigaki. Single Crystal Structure Study of Type I Clathrate $\text{K}_8\text{Zn}_4\text{Sn}_{42}$ and $\text{K}_8\text{In}_8\text{Sn}_{38}$. *J. Electron. Mater.*, 46:2765, 2017.
- ⁴⁵ Philip M. Morse. Diatomic Molecules According to the Wave Mechanics. II. Vibrational Levels. *Phys. Rev.*, 34:57–64, 1929.
- ⁴⁶ Manjeera Mantina, Adam C. Chamberlin, Rosendo Valero, Christopher J. Cramer, and Donald G. Truhlar. Consistent van der Waals Radii for the Whole Main Group. *The Journal of Physical Chemistry A*, 113(19):5806–5812, 2009.
- ⁴⁷ A. Bondi. van der Waals volumes and radii. *J. Phys. Chem.*, 68:441–451, 1964.
- ⁴⁸ M. Koza, L. Capogna, A. Leithe-Jasper, H. Rosner, W. Schnelle, H. Mutka, M. R. Johnson, C. Ritter, and Y. Grin. Vibrational dynamics of filled skutterudites $M_{1-x}\text{Fe}_4\text{Sb}_{12}$ ($M = \text{Ca}, \text{Sr}, \text{Ba}, \text{and Yb}$). *Phys. Rev. B*, 81:174302, 2010.
- ⁴⁹ B. C. Melot, R. Tackett, J. O’Brien, A. L. Hector, G. Lawes, R. Seshadri, and A. P. Ramirez. Large low-temperature specific heat in pyrochlore $\text{Bi}_2\text{Ti}_2\text{O}_7$. *Phys. Rev. B*, 79:224111, 2009.
- ⁵⁰ D. P. Shoemaker, R. Seshadri, M. Tachibana, and A. L. Hector. Incoherent Bi off-centering in $\text{Bi}_2\text{Ti}_2\text{O}_6\text{O}'$ and $\text{Bi}_2\text{Ru}_2\text{O}_6\text{O}'$: Insulator versus metal. *Phys. Rev. B*, 84:064117, 2011.